

1 The role of grain size and inoculum amount on biocrust formation by *Leptolyngbya*
2 *ohadii*

3 **Gianmarco Mugnai^{1a}, Federico Rossi^{1a*}, Sonia Chamizo^{1b}, Alessandra Adessi¹, Roberto De**
4 **Philippis¹**

5 ¹Department of Agricultural, Food, Environmental and Forestry Science and Technology -DAGRI,
6 University of Florence, via Maragliano 77, 50144 Florence, Italy

7 ^aCurrent address: Department of Food, Environmental and Nutritional Sciences (DeFENS),
8 University of Milan, via Luigi Mangiagalli 25, 20133 Milan, Italy

9 ^bCurrent address: Agronomy Department, University of Almeria, La Cañada de San Urbano s/n,
10 04120 Almeria, Spain

11

12 *Corresponding Author

13

14

15

16

17

18

19

20

21

22

23

24

25

26

27

28

29

30

31

32

33

Abstract

Cyanobacteria are widespread prokaryotic organisms that represent feasible biotechnological tools to set up valid approaches to counteract desertification. Their peculiar physiological traits, and their resilience to abiotic stresses, allows their application on abiotically constrained soils to trigger their stabilization. A successful cyanobacteria inoculation results in the formation of cyanobacterial biocrusts, complex microbial communities characterized by tangled filament meshes imbued in a matrix of self-secreted extracellular polysaccharides (EPS) that keep loose sediments and aggregates firmly in place. However, the capability to form stable cyanobacterial biocrusts is not common to all the species, and a mix of factors can hamper the success of the treatment, notably inoculum amount, and substrate characteristics.

The aim of this work was to assess the influence of inoculum quantity and substrate granulometry on the physical stability of cyanobacterial biocrusts induced by inoculating the strain *Leptolyngbya ohadii* in a microcosm experiment, under laboratory conditions. After applying three different initial inoculum amounts on two different sand granulometries (medium and coarse sand), we assayed aggregate stability, physical stability and surface hydrophobicity on the resulting biocrusts during a 30-day incubation. Also, the features and the role of the EPS synthesized by *L. ohadii* were studied following their isolation, characterization, and direct application on the sand. The two EPS fractions produced by the strain, one more soluble and easily released in the surrounding medium (released polysaccharides, RPS) and one solidly attached to the filaments (glycocalyx EPS, G-EPS), were separately tested.

Cyanobacterial biocrusts visibly formed in all the microcosms after 15 days. However, we observed a strong effect of sand granulometry in affecting aggregate stability and tensile strength, both of which appeared weaker on coarse sand. A higher amount of initial inoculum was necessary to produce stable biocrusts on coarse sand compared to medium sand. Also, we observed how the inoculation of EPS alone did not sort most of the significant effects that we detected by inoculating the whole culture, pointing at the importance of the action of the cyanobacterial filaments in soil conglomeration. However, a significant increase in physical stability was achieved by inoculating G-EPS on medium sand, suggesting the involvement of this fraction in biocrusts structuration.

This work analyzes for the first time the effects of the variable grain size and inoculum amount in the achievement of physically stable biocrusts by cyanobacteria inoculation. The results that we obtained are useful in improving and optimizing the process of biomass preparation and dispersion for future indoor and outdoor studies.

68
69
70
71
72
73
74
75
76
77
78
79
80
81
82
83
84
85
86
87
88
89
90
91
92
93
94
95
96
97
98
99
100
101

Keywords: biocrusts, inoculation, aggregate stability, tensile strength, RPS, G-EPS.

1. INTRODUCTION

Cyanobacteria are phototrophic prokaryotes commonly found in a wide array of habitats on Earth, in temperate and extreme climates, in marine and fresh waters and from soil to rocks (Rossi and De Philippis, 2015). Many cyanobacterial species can colonize arid and hyper-arid substrates, even affected by salt stress, at a temperature range of 45-70 °C, pH lower than 4-5 (with optimum between 7.5-10) and under severe drought (Singh et al., 2016). Several authors already described their capability to promote the stability of soil aggregates against breakdown by wetting and physical forces (Malam-Issa et al., 2007; Rogers and Burns, 1994). Also, the presence of cyanobacteria positively affects the level of soil organic carbon and influence water distribution (Chamizo et al., 2018b; Colica et al., 2014; Muñoz-Rojas et al., 2018; Singh et al., 2016). Owing to these features, some selected strains revealed effective inoculants in arid and hyper-arid environments to promote sand dune stabilization and desertification reversal (Lan et al., 2014; Li et al., 2014), in a technology known as cyanobacterization (D'Acqui, 2016). Cyanobacteria aggregate the sand by forming a dense and sticky network constituted by filaments and exopolysaccharides (EPS) that bind together sand particles, forming cyanobacterial biocrusts (or algal biocrusts). These early formations represent the incipient developmental phase of complex and ecologically relevant microbial communities known as biological soil crusts, whose impact on arid and hyper-arid environment has been widely discussed (Belnap and Weber, 2013; Bowker, 2007; Weber et al., 2015). In the crusting process, the release of cyanobacterial EPS in the surrounding environment has several important implications. Their amphiphilic and hygroscopic nature allows to maintain hydration and tolerate desiccation, they shield cells from excessive solar irradiation and from protozoan predation, protect from freezing and salt stress, while chelating and immobilizing nutrients from the surrounding environment (Li et al., 2001; Rossi et al., 2018; Rossi and De Philippis, 2015; Swenson et al., 2018). On the other hand, EPS regulate the attachment to surfaces by changing the hydrophobicity of the cyanobacterial filaments (Mazor et al., 1996), gluing unitary sand particles into cohesive biocrust layers (Malam Issa et al., 2001).

The choice of the most feasible cyanobacterial inoculants is a very important starting point before attempting any cyanobacterization treatment. Inoculants must fit with a given soil type and environmental conditions, so that a treatment is tailor-made for a specific environment to rehabilitate (Malam-Issa et al., 2007; Singh and Kaur, 2009). In this framework, the physiological characteristics of the strain are a very important factor impinging on its capability to survive and form stable biocrusts. For example, the gliding motility, typical of some species such as the model inoculant *Microcoleus vaginatus*, allows avoidance of strong sunlight and propulsion towards

136 increasing moisture gradient, away from surface-desiccation fronts (Garcia-Pichel and Pringault,
137 2001). The gliding process also allows a wider release of EPS, enhancing the crusting process
138 (Mugnai et al., 2018b). The chemical quality of EPS is highly related to their capability to glue
139 loose sand together (Attou et al., 1998; Hu et al., 2003; Malam Issa et al., 2001), although the
140 information on the most influential EPS features is still limited. The monosaccharide composition
141 and the molecular size of cyanobacterial EPS so far analyzed are highly variable, and generally
142 complex (Mugnai et al., 2018a; Pereira et al., 2009; Rossi and Philippis, 2016). Furthermore, EPS
143 features are significantly affected by nutrient levels (Mager and Thomas, 2010; Rossi and Philippis,
144 2016), water availability (Mugnai et al., 2018a), or soil type (Chamizo et al., 2018a), so that they
145 cannot be considered absolute for a given strain, but differing according to abiotic conditions
146 (Mugnai et al., 2018a). By determining variations in EPS chemical quality, environmental
147 parameters affect the crusting capability of cyanobacterial inoculants. Additional factors can
148 hamper or condition cyanobacteria establishment and biocrust formation. One is inoculum quality,
149 that include the amount, preparation and dispersion of the biomass. At the moment, standardized
150 protocols do not exist, and methodologies have been diverse (Hamdi, 1982; Rossi et al., 2017).
151 Other known factors impinging on cyanobacterization success are unfavorable soil pH, low P
152 levels, low water availability, and, importantly, granulometry of the substrate (Rossi et al., 2017;
153 Rozenstein et al., 2014). Rozenstein et al. (2014) found that cyanobacterial biocrusts develop more
154 rapidly on finer substrates, while they resulted patchy and discontinuous on coarse sand. However,
155 we have no indications concerning how substrate granulometry influences tensile strength and
156 aggregate stability of biocrusts. The large number of factors at play during biocrust formation
157 explains the highly variable responses so far registered by employing different inoculants, both in
158 desert environments and in agricultural settings (Rossi et al., 2017). Some inoculants only form thin
159 films at the soil surface, while others form crusts with aggregation and physical stability that are too
160 poor to withstand erosion events typical of arid and semiarid environments (Hu et al., 2002; Rossi
161 et al., 2017). Wind erosion can dismantle the incipient biocrust structure if its threshold friction
162 velocity does not exceed wind forces experienced in a given environment (Belnap and Gillette,
163 1998). A deeper knowledge on the paramount factors influencing inoculant establishment and stable
164 cyanobacterial biocrust formation is important to select novel and performing candidates and
165 employ them in the frame of optimized procedures. *Leptolyngbya ohadii* is a model strain that we
166 employed in a previous study (Mugnai et al., 2018b). Following an optimized inoculation protocol,
167 it revealed a very good crust former, useful for testing how the variation of different parameters
168 affect the cyanobacterization outcome. We utilized the strain to investigate how water availability
169 impinges on the physical characteristics of biocrusts, and on the chemical quality of EPS (Mugnai et

170 al., 2018b). The present work aims at an additional step forward, which is to employ *L. ohadii* to
171 investigate if and how the amount of initial inoculum and the granulometry of the substrate
172 influence several biocrust parameters, namely tensile strength, aggregate stability and surface
173 hydrophobicity. Expecting, by literature, a different inceptive colonization between coarse and fine
174 substrates, we concurrently hypothesized a significant difference in the physical stability of the
175 induced biocrusts. Additionally, the role of the EPS excreted by the strain on sand aggregation
176 process was also investigated.

177

178 **2. MATERIAL AND METHODS**

179

180 **2.1. Sand inoculation experiments**

181

182 *2.1.1 Organism and culture conditions*

183

184 *L. ohadii* was kindly provided by the Department of Plant and Environmental Sciences, The
185 Hebrew University of Jerusalem, Israel. It is a filamentous, non-heterocystous cyanobacterium
186 isolated from biocrusts collected in the Nizzana region of the Negev Desert, Israel (Ohad et al.,
187 2010; Raanan et al., 2016). Its morphological characteristics were first described in Mugnai et al.
188 (2018b). It does not produce an exocellular sheath when grown in liquid culture, although a more
189 condensed EPS fraction remains attached to the filament (hereafter referred to as “glycocalyx EPS”,
190 G-EPS) and one more soluble (hereafter referred to as “released polysaccharides”, RPS) is released
191 in the culture medium.

192 *L. ohadii* was grown in BG11 medium (Rippka, 1988) for 30 days in Pirex flasks in an orbital
193 incubator (INNOVA 44-R, New Brunswick) at a temperature of 30 °C, at low light intensity of 15
194 $\mu\text{mol photons m}^{-2} \text{s}^{-1}$ and a constant stirring of 100 rpm until reaching the stationary phase.

195

196 *2.2.2. Isolation and characterization of EPS from liquid culture*

197

198 RPS were isolated by centrifuging the culture at $4,000 \times g$ for 30 min at room temperature. The
199 supernatant was enclosed in nitrocellulose tubular dialysis membranes (Medicell International, 12-
200 14,000 MWCO) and dialyzed against 10 volumes of distilled water for 48 h under continuous
201 stirring, with two changes of water, and then concentrated by using an orbital evaporator at 35 °C.
202 G-EPS were extracted from the pellet obtained after RPS removal, washing the resulting pellet with
203 0.5% NaCl solution and then extracting it with 4 mL hot (80 °C) distilled water for 1 h. After

204 centrifuging at $4,000 \times g$ for 30 min, the G-EPS-containing supernatant was collected. Both RPS
205 and G-EPS were eventually lyophilized and used for macromolecular characterization.
206 Additionally, RPS and G-EPS were used to test their sole effect when applied to the sand, as
207 compared with the whole cyanobacterial biomass.

208 The monosaccharidic composition of the two fractions was determined by ion-exchange
209 chromatography (IEC) on dried EPS samples after hydrolyzation with trifluoroacetic acid according
210 to Mugnai et al. (2018b). Samples were analyzed by using a Dionex ICS-2500 ion exchange
211 chromatograph (Dionex, Sunnyvale, CA) equipped with an ED-50 detector with a gold-working
212 electrode, and a CarboPac PA1 column of 250 mm length and 4.6 mm internal diameter (Dionex,
213 Sunnyvale, CA). Chromatographic conditions were in accordance with Chen et al. (Chen et al.,
214 2014). Unknown sugars were identified by injecting several concentrations of standard
215 monosaccharides and plotting response area as function of concentration.

216 The apparent molecular weight (MW) was determined by Size-Exclusion Chromatography
217 (SEC). EPS were dissolved in deionized water and injected in a Varian Pro-Star liquid
218 chromatographer (Varian Inc., USA) equipped with two PolySep – GFC–P 6000 and 4000 columns
219 (Phenomenex, USA) connected in series, and a refractive index detector. The eluent was HPLC-
220 grade water at a working flow of 0.4 mL min^{-1} . Dextran at known MWs (2,000 kDa, 1,100 kDa, 410
221 kDa, 150 kDa, 50 kDa) purchased from Sigma Aldrich, was used as a reference standard to
222 determine MW classes according to retention time.

223

224 2.2.3. Sand inoculation with *L. ohadii* and with isolated EPS

225

226 Biomass and EPS (RPS and G-EPS) obtained from *L. ohadii* were inoculated in microcosms
227 constituted of Petri dishes of 92 mm (diameter) x 16 mm (depth), containing 80 g of sand
228 alternatively with a granulometry of 0.3 – 0.6 mm (henceforth medium sand, MS) or 0.8 – 1.25 mm
229 (henceforth coarse sand, CS). The sand was a commercial dried silica sand (VAGA s.r.l., Pavia,
230 Italy) with known chemical and mineralogical composition (Tab. S1) that was autoclaved twice
231 before use. The experimental design is summarized in Table S2. A total of 90 microcosms (45
232 microcosms containing MS and 45 microcosms containing CS) were prepared and divided in two
233 subsets (one to receive culture inoculum and one to receive EPS suspension) to serve in two
234 temporally separated experimental phases. In the first experimental phase, 36 microcosms, 18
235 containing MS and 18 containing CS, were inoculated with cyanobacterial biomass, preventively
236 treated according to Mugnai et al. (2018a, b). Briefly, the culture medium was removed by
237 centrifugation, trichomes fragmented with sterile tweezers, and eventually re-suspended in distilled

238 water in a volume to provide enough inoculum for all the microcosms. After determining the dry
239 weight (DW), the biomass was applied on the sand, drop by drop with a sterile 10 mL pipette, using
240 a “double spiral dispersion” inoculation methodology, i.e. applying the biomass following a first
241 spiral line and then by applying a second spiral in the empty spaces left on the sand by the first
242 spiral (see the sketch in Figure 2a). The inoculum was applied in volumes corresponding to 0.15,
243 0.45 and 0.75 mg cell dry weight (CDW)/cm², calculated based on cell DW, and considering
244 microcosm surface area. In addition, 12 microcosms (6 with MS and 6 with CS) were not inoculated
245 and served as control. In a second experimental phase, a total of 36 microcosms (half containing
246 MS and half containing CS were inoculated alternatively with RPS and G-EPS suspended in
247 deionized water, in amounts corresponding to 6.8, 13.5 and 27.1 µg EPS/cm². Such amounts
248 corresponded to the highest values of EPS contents detected in 30-day-old cyanobacterial biocrusts
249 induced in the first experimental phase by applying respectively the lowest, the intermediate and the
250 highest quantity of initial inoculum (see Tab. 4 and section 2.2.7 for EPS quantification method).
251 Six non-inoculated microcosms containing MS (3) and CS (3) served as control. Inoculated
252 microcosms and controls were incubated for 30 days in a plexiglass growth chamber under
253 controlled temperature (30°C), illumination (45 µmol photons m⁻² s⁻¹) and relative humidity (RH, 0
254 %) conditions. RH was monitored with a digital hygrometer (VWR, USA), having an accuracy of
255 5%. Every two days, 0.4 mm distilled water was sprayed over each microcosm, including the
256 control, according to Mugnai et al. (2018b). Microcosms inoculated with cyanobacterial biomass
257 (first experimental phase) were collected and analyzed 15 and 30 days. Microcosms with EPS
258 suspensions (second experimental phase) were collected only after 30 days.

259

260 *2.2.4. Spectral measurements*

261

262 Surface reflectance (SR) was used as a non-destructive measure of cyanobacterial biocrust
263 development (Rozenstein et al., 2014). SR was measured at the end of incubation (30 days) with an
264 Analytical Spectral Device (ASD) hand held portable spectroradiometer (ASD Inc., Boulder,
265 Colorado, USA), under constant light conditions. The instrument had a sampling interval of 3.5 nm
266 from 325 nm to 1075 nm and was equipped with an optic fiber which was placed 16 cm above the
267 soil sample, to measure the total surface of the microcosm. Before measurements, the
268 spectroradiometer was calibrated using a 99% Spectralon(r) panel. Two spectra were taken per
269 sample, each one consisting on the internal average of three individual spectra, resulting in six
270 pseudo-replicates that were averaged to obtain the mean spectrum for each sample. Then, the three
271 independent replicates per treatment were averaged to obtain the mean spectral curve per inoculum

272 amount and granulometry. All reflectance values were expressed proportional to the 99%
273 Spectralon standard. Data were acquired with the RS³ Spectral Acquisition Software on a laptop
274 connected to the spectroradiometer. After data collection, data pre-processing was performed by
275 removing noisy bands in the range between 325 and 400 nm and between 950 and 1075 nm and
276 later application of a cubic polynomial smoothing filter (Savitzky and Golay, 1964).

277 Spectral absorptions at specific wavelengths were extracted using the continuum removal
278 (CR) technique (Clark and Roush, 1984). This technique normalizes comparison between samples
279 by rationing the measured spectrum to the estimated reflectance of a common baseline which has a
280 value of 1.0. Values equal to 1.0 indicate no absorption, while values lower than 1.0 indicate the
281 presence of absorption features. The continuum-removal was computed using ENVI 4.3 (ITT VIS,
282 Boulder, CO, USA).

283

284 *2.2.5. Crust thickness and stability measurement*

285

286 The thickness of the cyanobacterial biocrusts was measured with a caliper after 30 days of
287 incubation. Aggregate stability (AS) of the cyanobacterial biocrusts was measured applying the
288 single water-drop test (Imeson and Vis, 1984). Biocrust aggregates were first sieved to 4.0 and 4.8-
289 mm size. Next, 0.1 g water drops were allowed to fall from 1 m height onto biocrust aggregates
290 placed on a 2.8-mm metal mesh sieve. The number of drops necessary to disrupt the aggregates was
291 counted and used as a stability index. For each sample, the final number of drops needed was
292 calculated as a mean of at least 15 instrumental replicates ($n = 15$).

293 Tensile strength was measured using a digital force gauge (Mark-10 Model M7-5, 25N,
294 Mark-10 Corp, USA) equipped with a cone tip (0.5mm length, 0.6mm diameter). Crusts were oven-
295 dried (40°C) for 4 h before each measurement. Samples were placed onto a lifting table that was
296 raised up until probe–soil contact produced biocrust break-down. The registered peak value
297 corresponded to the breaking point of the crust aggregates, and to their tensile strength. Five
298 instrumental replicates were conducted for each sample ($n = 5$).

299

300 *2.2.6. Soil water repellency*

301

302 Surface water repellency (SWR) of induced cyanobacterial biocrusts was assessed by the water
303 drop penetration time (WDPT) test and repellency index (RI) measurement.

304 WDPT test was performed on the samples after 15 and 30 days of incubation, according to
305 Bisdom et al. (1993). A drop of distilled water of 50 (± 5) μL was released from a height of 10 mm

306 on the biocrust surface, and the time for complete drop infiltration was recorded. For each sample,
307 the final infiltration time was calculated as a mean of 10 instrumental repetitions ($n = 10$). Samples
308 were considered as wettable when WDPT < 5 s, slightly water repellent when WDPT ranged
309 between 5 and 60 s, and strong water repellent when > 60 s (Bisdorn et al., 1993).

310 RI was determined on the samples after 15 and 30 days of incubation according to Mugnai et
311 al. (2018a), utilizing a miniaturized tension infiltrometer (Lichner et al., 2013). After calculating the
312 sorptivity of distilled water and 95 % ethanol at – 2 cm head pressure, RI was calculated applying
313 the following formula:

$$RI = 1.95 \sqrt{\frac{S_E}{S_W}}$$

314 where S_E is the sorptivity of 95 % ethanol and S_W is the sorptivity of distilled water, while the factor
315 1.95 accounts for differences in viscosity and surface tension between the two liquids (Tillman et
316 al., 1989). A soil with a $RI = 1$ (i.e. where $S_E = S_W$) is considered non-repellent, whereas a
317 subcritical repellency is characterized by RI values greater than 1 and lower than 1.95. Values
318 greater than 1.95 indicate a critically water repellent soil.

319
320 *2.2.7. Extraction and quantification of EPS in cyanobacterial biocrusts*

321
322 EPS were extracted and quantified in the biocrusts after 15 and 30 days since inoculation according
323 to previously set protocols (Rossi et al., 2018). 20 g of dry homogenized crust were suspended for
324 15 min in distilled water and then centrifuged at 4000 x g for 30 min at 4 °C to recover the soluble
325 EPS fraction. Then, the EPS fraction more condensed around sediments and filaments was extracted
326 by treating the pellet with 0.1 M Na₂EDTA for 16 h at room temperature, then recovering it by
327 centrifuging at 4000 x g for 30 min at 4°C. Finally, the two fractions were blended and quantified as
328 total EPS. The quantification was done by the phenol-sulfuric acid assay (Dubois et al., 1956).
329 Briefly, 1 ml 5% phenol was added to the sample, followed by the addition of 5 ml H₂SO₄. The mix
330 was incubated at room temperature for 10 min, water-cooled for 15 min and then analyzed
331 spectrophotometrically at 488 nm. D-glucose at different concentrations was used as a reference
332 standard.

333

334 **3. STATISTICAL ANALYSIS**

335

336 All the analysis was conducted in experimental triplicates ($N = 3$); a minimum number of three
337 instrumental replicates was always conducted for each measurement ($n = 3$). To analyze whether
338 the results were significantly different, data were treated using one-way analysis of the variance
339 (ANOVA) at 95% of the significance, followed by Tukey's honest significance difference (HSD)
340 post-hoc test. Results were considered significant at $P \leq 0.05$. Prior to ANOVA, data Independence
341 (Pearson's Chi-square test), normal distribution (D'Agostino-Pearson normality test), and
342 homogeneity of variance (Bartlett's test) were assessed. To correlate parameters, linear regression
343 analyses were performed, and r^2 and P values are reported for each case. Statistical analysis was
344 performed using GraphPad Prism version 6.00 (GraphPad software, USA).

345

346 **4. RESULTS**

347

348 **4.1. Monosaccharide composition and apparent molecular weight of EPS from *L. ohadii***

349

350 Overall, 13 different monosaccharide moieties were detected by analyzing the EPS produced by *L.*
351 *ohadii* in liquid culture (Fig. 1a). IEC unveiled a marked difference between G-EPS and RPS. The
352 former fraction was dominated by glucose (accounting for 48% of the components), characterized
353 by higher content of ribose (21%) than RPS, and slightly higher amounts of galacturonic acid (5%).
354 On the other hand, RPS contained glucuronic acid as the dominant moiety (accounting for nearly
355 40% of the detected constituents), had higher contents of rhamnose, galactosamine, galactose,
356 mannose and xylose, than G-EPS.

357

[Near Figure 1]

358

359 SEC revealed that the two EPS fractions were polydisperse polymers, constituted by
360 macromolecules having a large MW distribution. However, while G-EPS showed fractions
361 distributed in four MW classes ranging between 2,000 kDa and 50 kDa, RPS showed a predominant
362 (71%) fraction having an apparent MW between 2,000 kDa and 1,100 kDa (Fig.1 b).

363

364 **4.2. Effects of the inoculation of *L. ohadii* biomass**

365

366 *4.2.1 Effects on cyanobacterial biocrust development and stability*

367

368 The “double spiral dispersion” methodology (sketched in Fig. 2a) allowed an even distribution of
369 the biomass on the microcosm surface (Fig. 2b), determining the formation of cyanobacterial

370 biocrusts on MS (Fig. 2c) and CS (Fig. 2d) with a significant thickness on both substrates (Fig. 2e,
 371 f). The thickness was in accordance with initial inoculum amount and influenced by substrate
 372 granulometry (Tab. 1).

373

374

[Near Fig. 2]

375 On CS, a consistent thickness was observed only in the crusts obtained by applying the intermediate
 376 and the highest inoculum amounts, while in those obtained by applying the lowest amount, crusts
 377 were very thin and fragile, not allowing to obtain solid measurements. On MS, a coherent crust
 378 (7.03 ± 0.41 mm thick) was observed even applying the lowest amount of inoculum (Tab. 1). The
 379 thickness increased with the increase of the inoculum amount, showing comparable values in the
 380 biocrusts obtained by applying 0.45 and 0.75 mg CDW/cm².

381

382 **Table 1.** Thickness of cyanobacterial biocrusts measured at t = 30 with a caliper. MS: medium sand (granulometry 0.3
 383 – 0.6 mm); CS: coarse sand (granulometry 0.8 – 1.25 mm). Different letters indicate significant differences (P < 0.05)
 384 between the values employing different inoculum concentration. – absence of a measurable thickness. Values are
 385 expressed as mean \pm (SD).

Sand Granulometry		MS			CS			
Inoculum (mg CDW/cm ²)	Control	0.15	0.45	0.75	Control	0.15	0.45	0.75
Thickness (mm)	-	7.03 ^b (0.41)	7.85 ^a (0.75)	8.48 ^a (0.50)	-	-	7.33 ^b (0.73)	8.53 ^a (0.75)

386

387 Surface reflectance analysis at t = 30 d showed that cyanobacterial biocrust development darkened
 388 the surface and led to a decrease in reflectance in the visible (VIS) region (400-700 nm) compared
 389 to controls. The spectral curve was characterized by low reflectance in the blue region and
 390 increasing values towards the green and red regions, followed by a steeper increase in reflectance
 391 near the infrared region (700-950 nm; Fig. 3a, b). On MS, reflectance was lower in the biocrusts
 392 induced by inoculation with higher inoculum amounts (0.45 and 0.75 mg CDW/cm²) than in those
 393 with low amounts (0.15 mg CDW/cm²), and controls. Differences between control and inoculated
 394 soils were also reflected in the absorption at 680 nm due to chlorophyll *a* content. This absorption
 395 peak was absent in the controls and present in the inoculated sand, showing an increasing depth as
 396 the increasing initial inoculum amount increased (Fig. 3c, d). Another absorption peak was
 397 observed at 500 nm in both control and inoculated soils associated to the presence of iron oxides in
 398 the studied sandy substrates (Tab. S1), which can interfere with absorption by carotenoids, which
 399 also absorb at 500 nm (Weber et al., 2008).

400

401

[Near Figure 3]

402

403 Stability of biocrust aggregates was very low, with only less than five drops needed to break down
 404 the aggregates. However, we found some differences in aggregate stability among the biocrusts
 405 induced by the different inoculum concentrations on the MS. With this granulometry, after 30 days
 406 of incubation, the number of water droplets needed to disperse aggregates increased significantly
 407 according to the amount of initial inoculum (Tab. 2). On the other hand, cyanobacterial biocrusts on
 408 CS presented aggregates that were too weak to give consistent values when applying this method of
 409 analysis.

410

411 **Table 2.** Aggregate Stability (AS, expressed as the number of drops needed to disperse sand aggregates) and
 412 tensile strength, expressed as Maximum Penetration Resistance (MPR), expressed in kPa, of cyanobacterial
 413 biocrusts developed on MS and CS. AS was measured at $t = 15$ d and $t = 30$ d. Tensile strength was
 414 measured at $t = 30$ d. Different small letters indicate significant differences ($P < 0.05$) between the AS or the
 415 tensile strength values obtained employing different inoculum concentration. Dash (-) indicates an AS under
 416 the detection limit of the method. Values are expressed as mean \pm (SD)

Sand type		MS				CS			
Inoculum (mg DW/cm ²)		Control	0.15	0.45	0.75	Control	0.15	0.45	0.75
AS (average number of drops)	15d	-	-	3.40 ^c (0.39)	3.78 ^b (0.50)	-	-	-	-
	30d	-	2.45 ^d (0.12)	3.36 ^{bc} (0.22)	4.11 ^{ab} (0.39)	-	-	-	-
MPR [kPa]	30 d	1.70 ^c (0.09)	1.49 ^c (0.53)	7.59 ^b (1.74)	13.74 ^a (2.45)	2.37 ^b (0.99)	1.66 ^b (0.22)	1.22 ^b (0.91)	6.19 ^a (1.93)

417

418 Tensile strength of the biocrusts, measured at $t = 30$ depended upon sand type and inoculum amount
 419 (Tab. 2). On MS, cyanobacterial biocrusts showed a tensile strength that increased with the increase
 420 on inoculum amount. On CS, while no significant increase was observed between applying the
 421 lowest and the intermediate inoculum amount, a significantly increased tensile strength (from 1.22
 422 ± 0.91 to 6.19 ± 1.93 kPa) was detected in the biocrusts obtained by applying the highest inoculum
 423 amount.

424

425 4.2.2 Effects on surface water repellency (SWR)

426

427 At $t = 15$ d, WDPT test revealed a strong SWR of cyanobacterial biocrusts obtained by applying
 428 0.45 and 0.75 mg CDW/cm² of inoculum on both MS and CS (Tab. 3). No SWR was revealed by
 429 WDPT test with the application of only 0.15 mg CDW/cm². From $t = 15$ d to $t = 30$ d, values
 430 decreased significantly in all the cases.

431
432
433
434
435
436

Table 3. Water drop penetration time test (WDPT) and repellency index (RI) of induced cyanobacterial biocrusts. Different letters indicate a significant difference among the treatments, and between t = 15 d and t = 30 d of incubation, on each sand type. Values are expressed as mean ± (SD).

Sand Granulometry		MS				CS			
Inoculum (mg CDW/cm ²)		Control	0.15	0.45	0.75	Control	0.15	0.45	0.75
WDPT [sec]	15d	0.0 ^d (0.01)	0.0 ^d (0.01)	10.98 ^{bc} (3.67)	>20 ^a (7.64)	0.0 ^d (0.01)	0.0 ^d (0.01)	6.06 ^c (1.16)	>20 ^a (6.26)
	30d	0.0 ^d (0.01)	0.0 ^d (0.01)	1.45 ^{cd} (1.09)	9.71 ^b (3.51)	0.0 ^d (0.01)	0.0 ^d (0.01)	7.55 ^{bc} (6.54)	10.51 ^b (9.11)
RI	15d	1.04 ^c (0.11)	1.91 ^c (0.5)	12.09 ^{ab} (3.3)	14.23 ^a (1.94)	0.88 ^b (0.43)	3.54 ^b (1.50)	>20 ^a (0.67)	>20 ^a (2.69)
	30d	1.14 ^c (0.16)	1.24 ^c (0.1)	7.22 ^b (4.06)	7.26 ^b (0.77)	0.86 ^b (0.62)	2.11 ^b (0.53)	1.82 ^b (0.52)	1.89 ^b (0.47)

437
438
439
440
441
442
443
444
445

At t = 15 d, RI analysis showed that cyanobacterial biocrusts on MS induced by applying 0.45 and 0.75 mg CDW/cm² biomass showed a critical SWR (RI > 1.95), whereas a sub-critical one was observed applying 0.15 mg CDW/cm². At t = 30 d, cyanobacterial biocrusts still maintained a critical or subcritical repellency value, despite a general decline in the values. On CS, although at t = 15 d biocrusts showed a critical SWR according to RI values, only sub-critical values were found for all the treatments at t = 30 d. After 30 d, a significant increase of RI was observed from applying the lowest, the intermediate and the higher inoculum amounts.

4.2.3 Effects on EPS contents in cyanobacterial biocrusts

446
447
448
449
450
451
452

Total EPS contents of cyanobacterial biocrusts, determined at t = 15 d and t = 30 d, increased showing a positive correlation with the amount of initial inoculum in both MS ($r^2=0.98$, $P = 0.07$ and $r^2 = 0.98$, $P = 0.06$ for t = 15 and t = 30 d, respectively) and on CS ($r^2 = 0.98$, $P = 0.09$ and $r^2 = 0.97$, $P = 0.1$ for t = 15 d and t = 30 d, respectively). The highest EPS content in biocrusts both in MS and in CS was detected at t = 15 d (Tab. 4).

453
454
455
456
457

Table 4. EPS content in cyanobacterial biocrusts (expressed as µg EPS per g biocrust) that were induced by inoculating *L. ohadii* at three different inoculum amounts, expressed as mg cell dry weight (CDW) per square centimeter. Presented data were treated by subtracting the values detected in non-inoculated microcosms (controls), to correct for background noise. Different letters indicate a significant difference ($P <$

458 0.05) in EPS contents by applying different inoculum amounts. MS, medium sand; CS, coarse sand. Values
 459 are expressed as mean \pm (SD).

Sand Granulometry		MS			CS		
inoculum (mg CDW/cm ²)		0.15	0.45	0.75	0.15	0.45	0.75
EPS μg [g biocrust] ⁻¹	15d	3.67 ^d (0.77)	13.27 ^{bc} (1.97)	27.86 ^a (1.39)	2.43 ^{dc} (1.47)	11.80 ^{bc} (1.26)	25.95 ^a (3.57)
	30d	3.45 ^d (0.81)	7.84 ^d (1.46)	15.28 ^b (2.58)	3.48 ^{dc} (0.41)	7.94 ^c (2.17)	15.65 ^b (1.79)

460
461

462 4.3 Effects of the sole EPS application

463

464 The application of pure EPS obtained from liquid culture did not produce any significant effect on
 465 AS, nor statistically significant variation of SWR. Values of RI lower than 1 (Table 3S) and values
 466 of WDPT < 5 sec (data not shown) were always found at t = 30 d. However, when the G-EPS
 467 solution was applied on MS, an increase in tensile strength was detected as the applied G-EPS
 468 concentration increased, while no significant effects were observed by applying RPS suspension
 469 (Table 5). On the contrary, G-EPS and RPS application on CS never affected the surface tensile
 470 strength, which showed values not statistically different from the control.

471

472 **Table 5.** Tensile strength (expressed in kPa) measured after 30 days on MS and CS microcosms following
 473 G-EPS and RPS application isolated from liquid culture of *L. ohadii*. Different letters indicate significant
 474 differences ($P < 0.05$) between the values obtained employing different EPS concentrations. MS, medium
 475 sand; CS, coarse sand. Values are expressed as mean \pm (SD).

476

Sand Granulometry		MS				CS			
EPS (μg/cm ²)		Control	6.80	13.54	27.09	Control	6.80	13.54	27.09
MPR [kPa]	RPS	1.70 ^a (0.11)	2.44 ^a (0.14)	1.69 ^a (0.56)	1.93 ^a (0.24)	2.12 ^a (0.55)	2.57 ^a (0.57)	2.32 ^a (0.67)	3.53 ^a (0.72)
	G-EPS	1.70 ^c (0.11)	2.63 ^{bc} (0.50)	3.07 ^b (0.56)	5.27 ^a (0.35)	2.12 ^a (0.55)	2.46 ^a (0.92)	2.90 ^a (0.19)	3.15 ^a (0.01)

477

478

479 5. DISCUSSION

480

481 In this work, we confirmed the marked capability of *L. ohadii* to form stable cyanobacterial
 482 biocrusts on sandy substrates. The inoculation was not supported by any type of nutrient addition,

483 nor by any pretreatment with stabilizing agents or tackifiers. Although we observed crust formation
484 on both sand types, the grain size of the substrate and initial inoculum concentration significantly
485 affected thickness, hydrophobic properties and physical stability of cyanobacterial biocrusts.

486 Overall, the strain more easily formed cyanobacterial biocrusts on MS than on CS. The
487 lowest inoculum amount (0.15 mg CDW/cm^2) did not induce cyanobacterial biocrusts with a
488 measurable thickness and tensile strength on CS; however, such amount was enough on MS.
489 Cyanobacterial biocrusts on CS also showed a very poor particle aggregation. Although aggregates
490 were visible, they resulted so fragile that the number of drops necessary to disrupt the aggregates
491 was very low, not allowing obtaining significant and reliable values for AS. On the other hand, the
492 same crusts presented a significant tensile strength when the highest inoculum amount was applied
493 (0.75 mg CDW/cm^2), indicating this as the sole inoculum amount determining a significant effect
494 on CS (Table 2). The impact of different initial inoculum amount and sand grain size on biocrust
495 formation was also supported by SR results. A significant reduction in albedo due to surface
496 darkening owing to biocrust development was observed, although only by applying 0.45 or 0.75 mg
497 CDW/cm^2 on MS, and 0.75 mg CDW/cm^2 on CS (Figure 3). It was already evidenced how finer
498 substrates are more supportive to cyanobacterial biocrust colonization (Rozenstein et al., 2014). The
499 larger pore spaces between the grains on CS arguably hindered the spatial spreading of
500 cyanobacterial filaments by imposing the organism a more elaborated development process to fill
501 the voids, surround sand particles and then connect them together steadily. This was recently
502 evidenced by scanning electron microscopy for *Phormidium ambiguum* and *Scytonema javanicum*
503 growing on sandy soils (Chamizo et al., 2018a). While on sandy loam soils the filaments formed a
504 very packed filament network embedding sediments, on sandy soil the biocrusts structure showed
505 frequent air spaces between sand grains which become entangled in a network. In addition to the
506 decrease of albedo by surface darkening, biocrust development was supported by the common
507 absorption feature around 670 nm due to chlorophyll *a*, which was absent in the control sand
508 (Weber et al., 2008). Moreover, this absorption increased as the inoculum amount increased (Fig. 3c
509 and Fig. 3d) demonstrating that crust spectral features can be used to assess crust development. To
510 this regard, a recent paper has shown a strong correlation between chlorophyll content and different
511 spectral indices in natural and induced biocrusts, supporting the possibility of using non-destructive
512 soil surface reflectance measurements for chlorophyll quantification in biocrusts (Román et al.,
513 2019).

514 We provided supporting evidence that increasing the initial inoculum can promote an
515 effective biocrusts formation on CS. The application of a higher concentration of initial biomass
516 reflected also in increased EPS amounts in cyanobacterial biocrusts (Table 4). Beside contributing

517 to sand gluing and stabilization, EPS most likely contributed to the increase in SWR, according to
518 RI and WDPT test values (Table 3). This aspect was already observed in cyanobacterial biocrusts
519 induced employing this strain (Mugnai et al., 2018b). This is important to a physiological level in
520 hot drylands, as it extends water permanence in the first mm of soil to the availability of the
521 microbial community, counteracting water loss by evaporation. In contrast, inoculation of other
522 cyanobacterial strains such as *P. ambiguum* and *S. javanicum* on sandy soils was found to not
523 significantly change surface hydrophobicity (Chamizo et al., 2018a). The presence of charged
524 groups on the soluble EPS fractions determines the formation of viscous aqueous solutions (De
525 Philippis and Vincenzini, 1998) that have more difficulty in seeping through the sand. It was
526 previously reported that the EPS extracted from the biocrusts obtained by inoculating *L. ohadii* is
527 characterized by a significant amount of galacturonic acid, especially in the fractions loosely bound
528 to sand grains and filaments (Mugnai et al., 2018b). The complex nature of EPS synthesized by the
529 strain is most likely a significant driver in the stabilization of the sand. In liquid culture, the
530 polysaccharide is partly released in the culture medium (named released polysaccharide, RPS), and
531 partly remain attached to the filaments (named glycocalyx polysaccharide, G-EPS), although not
532 structured like a sheath or a capsule. By characterizing the two fractions for the first time, we
533 observed differences in composition and MW distribution profiles. IEC revealed that although both
534 fractions owned a similar richness in the number of different types of monosaccharides, they
535 showed significant differences in their molar percentages. Notably, G-EPS resulted richer in
536 glucose and ribose, but significantly poorer in rhamnose, galactose, mannose and xylose, than RPS.
537 On the other hand, in RPS we detected marked levels (roughly 40%) of glucuronic acid, a
538 carboxylic sugar that gives a strong negative charge to the polymer. The two fractions were also
539 different in MW distribution profiles. RPS were prominently constituted by high MW polymers, of
540 a molecular size between 2,000 and 1,100 kDa, while the G-EPS showed a MW distribution with
541 three prevalent MW ranges: one between 2,000 and 1,000 kDa, a second between 410 and 150 kDa,
542 and a third between 150 and 50 kDa. Such a diverse monosaccharide composition and MW
543 distribution supports the existence of different supra-structures, and different capabilities to interact
544 with the surrounding environment (Delattre et al., 2016). In the attempt to isolate only the
545 contribute of EPS to biocrust formation, we applied alternatively G-EPS and RPS suspensions to
546 microcosms containing MS and CS, in concentrations corresponding to those detected in
547 cyanobacterial biocrusts induced by applying the three biomass concentrations. EPS application
548 never resulted in the formation of stable aggregates, nor in detectable variations in SWR. This result
549 enlightens how the sole presence of EPS would not suffice to explain most of what we observed
550 concerning SWR, AS and tensile strength of the cyanobacterial biocrusts without considering the

551 major contribution given by the cyanobacterial filaments. The creation of a filament network is thus
552 confirmed as a prerequisite to surface biological crusting (Chamizo et al., 2018b). However, we
553 found a significant increase in the surface tensile strength in MS microcosms when applying the
554 highest content of G-EPS, while no similar effect was observed employing RPS. We observed that
555 the same amount of G-EPS was not enough to trigger the same effect on CS. The larger pore spaces
556 in CS compared to MS, as previously discussed, probably limited the effect of EPS addition.
557 However, the significant effect that we detected on MS after G-EPS addition suggests this EPS
558 fractions as the most clearly contributing to sand structuration, although it was effective only on one
559 sand type. It is hazardous to try to link EPS chemical composition to their behavior without
560 information on the macromolecular secondary and tertiary structures. However, the detection of a
561 dominant presence of glucose in G-EPS, combined with a large variety of sugar types, support the
562 findings of Hu et al. (2003) that these characteristics are positively related with a stronger sand
563 stabilizing capability. It was previously discussed how the presence of hydrophobic fractions
564 enhances the capability of adhering to solid surfaces (Rossi et al., 2018). Also, G-EPS showed to be
565 a more polydisperse polymer than RPS, being constituted of fractions belonging to different MW
566 ranges. The majority (80%) of the characterized cyanobacterial EPS has an apparent MW of at least
567 1,000 kDa (Rossi and De Philippis, 2015). It is possible that the synthesis of EPS constituted by
568 different fractions with different MWs is a factor enhancing the sand aggregating capability, better
569 adapting to the uneven porosity of a coarser substrate. Indeed, Hu et al. (2003) demonstrated that
570 the presence of high MW polysaccharides is not necessarily related to a better sand stabilization.
571 The authors showed how *Microcoleus vaginatus*, a known natural cyanobacterial biocrust former
572 often employed in inoculation studies, secretes an EPS with a MW of 380 kDa, and displays a
573 higher sand stabilizing capability than *Nostoc* sp., employed in the same experiment, which
574 produced an EPS with a MW of 460 kDa. On the other hand, *L. ohadii* synthesize RPS prominently
575 characterized by macromolecules with an apparent MW of 1,000-2,000 kDa, and a marked content
576 of glucuronic acid. Due to their higher hydrophilic characteristics, RPS contribute to bind and retain
577 water molecules and nutrients (Rossi et al., 2012), likely playing the role of a selective filter and
578 sustaining the strain in adverse stressing conditions (Swenson et al., 2018). The MW distribution of
579 the two EPS fractions from *L. ohadii* is consistent with what we observed in a previous study in
580 which we analyzed the soluble and the more condensed EPM fractions directly extracted from *L.*
581 *ohadii* biocrusts. While the soluble EPM fraction was highly characterized by polymers with a MW
582 > 1,100 kDa, the more condensed, less soluble and structural EPM fraction was polydisperse
583 (Mugnai et al., 2018b). Contrastingly, a recent study analyzing the same aspects in cyanobacterial
584 crusts induced by inoculating *P. ambiguum* and *S. javanicum* described a different scenario. The

585 more hydrophobic EPM fraction, more firmly attached to soil particles, was mainly composed of
586 high MW molecules (1,100-2,000 kDa) while the more hydrophilic, which is released in the
587 surrounding environment, was composed of low MW sugars (< 50 kDa) (Chamizo et al., 2018a).
588 However, *L. ohadii* demonstrated a higher sand aggregation capability than *P. ambiguum* and *S.*
589 *javanicum* which produced biocrusts with a lower tensile strength on a sandy substrate (Chamizo et
590 al., 2018b). It is also possible that the employment of a strain capable of gliding allowed a wider
591 distribution of EPS in the sand, possibly enhancing sand fixation. Gliding strains migrate
592 hydrotactically (Garcia-Pichel and Pringault, 2001), or phototactically according to other sources
593 (Wilde and Mullineaux, 2017), horizontally and/or vertically (Nadeau et al., 1999), leaving behind a
594 trail of sticky polysaccharidic material (Hoiczyk, 2000) constituted both by G-EPS and RPS. We
595 previously deduced the capability of *L. ohadii* to move downwards in the microcosms, allowing a
596 vertical distribution of the cementing biomaterial, contributing to determine cyanobacterial
597 biocrusts with a notable thickness compared to other inoculants (Mugnai et al., 2018b).

598 In conclusion, we demonstrated how the evaluation of the optimal amount of biomass to
599 apply is key in the success of inoculum establishment on the sand, and the development of
600 cyanobacterial biocrusts. This is particularly important when treating substrates with varying
601 granulometry in which coarse particles abound, as compared to finer substrates. We advise to apply
602 an inoculum of at least 0.75mg CDW/cm² of biomass when inoculating coarse substrates. The
603 increase of inoculum amount coincided with the presence of a higher EPS content in the sand,
604 which contributes to sand fixation. We also underlined the more prominent role of G-EPS fraction,
605 in other strains organized as sheaths or capsules around the trichomes, in sand fixation. Further
606 studies are needed to provide further confirmation of our observation that the large content of
607 glucose, the low relative abundance of uronic acids, and the polydisperse MW of G-EPS can be
608 considered markers of a propensity of the strain to develop consistent cyanobacterial biocrusts. On
609 the other hand, RPS, more hydrophilic, are probably more involved in determining SWR. To obtain
610 consistent cyanobacterial biocrusts, EPS excretion must be coupled with the creation of a filament
611 network. Finally, the capability of the strain to glide seems to positively affect the strain
612 performance.

613

614 **ACKNOWLEDGEMENTS**

615

616 The authors wish to acknowledge Prof. Aaron Kaplan, the Hebrew University of Jerusalem, for
617 providing the strain *Leptolyngbya ohadii*. The authors also wish to thank Lisa Cangioli, Matilde
618 Ciani, Chiara Pastacaldi and Andrea Simiani (DAGRI, University of Florence) for the help in some

619 of the analytical procedures, and Xiangjun Zhou (School of Resources and Environmental Science,
620 Wuhan University) for the help with some of the instrumental analysis. Sonia Chamizo was
621 supported by the Hipatia postdoctoral fellowship funded by the University of Almería.

622

623 **6. REFERENCES**

- 624 Attou, F., Bruand, A., Le Bissonnais, Y., 1998. Effect of clay content and silt—clay fabric on
625 stability of artificial aggregates. *Eur. J. Soil Sci.* 49, 569–577.
626 <https://doi.org/10.1046/j.1365-2389.1998.4940569.x>
- 627 Belnap, J., Gillette, D. A., 1998. Vulnerability of desert biological soil crusts to winderosion: the
628 influences of crust development, soil texture, and disturbance. *J. Arid Environ.* 39, 133-142.
629 <https://doi.org/10.1006/jare.1998.0388>
- 630 Belnap, J., Weber, B., 2013. Biological soil crusts as an integral component of desert environments.
631 *Ecol. Process.* 2, 11.
- 632 Bisdorf, E.B.A., Dekker, L.W., Schoute, J.F.Th., 1993. Water repellency of sieve fractions from
633 sandy soils and relationships with organic material and soil structure. *Geoderma*,
634 *International Workshop on Methods of Research on Soil Structure/Soil Biota*
635 *Interrelationships* 56, 105–118. [https://doi.org/10.1016/0016-7061\(93\)90103-R](https://doi.org/10.1016/0016-7061(93)90103-R)
- 636 Bowker, M.A., 2007. Biological soil crust rehabilitation in theory and practice: an underexploited
637 opportunity. *Restor. Ecol.* 15, 13–23.
- 638 Chamizo, S., Adessi, A., Mugnai, G., Simiani, A., De Philippis, R., 2018a. Soil Type and
639 Cyanobacteria Species Influence the Macromolecular and Chemical Characteristics of the
640 Polysaccharidic Matrix in Induced Biocrusts. *Microb. Ecol.* [https://doi.org/10.1007/s00248-](https://doi.org/10.1007/s00248-018-1305-y)
641 [018-1305-y](https://doi.org/10.1007/s00248-018-1305-y)
- 642 Chamizo, S., Mugnai, G., Rossi, F., Certini, G., De Philippis, R., 2018b. Cyanobacteria Inoculation
643 Improves Soil Stability and Fertility on Different Textured Soils: Gaining Insights for
644 Applicability in Soil Restoration. *Front. Environ. Sci.* 6.
645 <https://doi.org/10.3389/fenvs.2018.00049>
- 646 Chen, L., Rossi, F., Deng, S., Liu, Y., Wang, G., Adessi, A., De Philippis, R., 2014.
647 Macromolecular and chemical features of the excreted extracellular polysaccharides in
648 induced biological soil crusts of different ages. *Soil Biol. Biochem.* 78, 1–9.
649 <https://doi.org/10.1016/j.soilbio.2014.07.004>
- 650 Clark, R.N., Roush, T.L., 1984. Reflectance spectroscopy: Quantitative analysis techniques for
651 remote sensing applications. *J. Geophys. Res. Solid Earth* 89, 6329–6340.
652 <https://doi.org/10.1029/JB089iB07p06329>
- 653 Colica, G., Li, H., Rossi, F., Li, D., Liu, Y., De Philippis, R., 2014. Microbial secreted
654 exopolysaccharides affect the hydrological behavior of induced biological soil crusts in
655 desert sandy soils. *Soil Biol. Biochem.* 68, 62–70.
656 <https://doi.org/10.1016/j.soilbio.2013.09.017>
- 657 D'Acqui, L.P., 2016. Use of Indigenous Cyanobacteria for Sustainable Improvement of
658 Biogeochemical and Physical Fertility of Marginal Soils in Semiarid Tropics, in: Arora,
659 N.K., Mehnaz, S., Balestrini, R. (Eds.), *Bioformulations: For Sustainable Agriculture*.
660 Springer India, pp. 213–232. https://doi.org/10.1007/978-81-322-2779-3_12
- 661 Delattre, C., Pierre, G., Laroche, C., Michaud, P., 2016. Production, extraction and characterization
662 of microalgal and cyanobacterial exopolysaccharides. *Biotechnol. Adv.* 34, 1159–1179.
663 <https://doi.org/10.1016/j.biotechadv.2016.08.001>
- 664 Dubois, M., Gilles, K.A., Hamilton, J.K., Rebers, Pa., Smith, F., 1956. Colorimetric method for
665 determination of sugars and related substances. *Anal. Chem.* 28, 350–356.

666 Hamdi, Y.A., 1982. Application of nitrogen-fixing systems in soil improvement and management.
667 Food & Agriculture Org.

668 Hoiczuk, E., 2000. Gliding motility in cyanobacteria: observations and possible explanations. Arch.
669 Microbiol. 174, 11–17. <https://doi.org/10.1007/s002030000187>

670 Hu, C., Liu, Y., Paulsen, B.S., Petersen, D., Klaveness, D., 2003a. Extracellular carbohydrate
671 polymers from five desert soil algae with different cohesion in the stabilization of fine sand
672 grain. Carbohydr. Polym. 54, 33–42. [https://doi.org/10.1016/S0144-8617\(03\)00135-8](https://doi.org/10.1016/S0144-8617(03)00135-8)

673 Hu, C., Liu, Y., Paulsen, B.S., Petersen, D., Klaveness, D., 2003b. Extracellular carbohydrate
674 polymers from five desert soil algae with different cohesion in the stabilization of fine sand
675 grain. Carbohydr. Polym. 54, 33–42.

676 Hu, C., Liu, Y., Zhang, D., Huang, Z., Paulsen, B.S., 2002. Cementing mechanism of algal crusts
677 from desert area. Chin. Sci. Bull. 47, 1361–1368. <https://doi.org/10.1360/02tb9301>

678 Imeson, A.C., Vis, M., 1984. Assessing soil aggregate stability by water-drop impact and ultrasonic
679 dispersion. Geoderma 34, 185–200. [https://doi.org/10.1016/0016-7061\(84\)90038-7](https://doi.org/10.1016/0016-7061(84)90038-7)

680 Lan, S., Zhang, Q., Wu, L., Liu, Y., Zhang, D., Hu, C., 2014. Artificially Accelerating the Reversal
681 of Desertification: Cyanobacterial Inoculation Facilitates the Succession of Vegetation
682 Communities. Environ. Sci. Technol. 48, 307–315. <https://doi.org/10.1021/es403785j>

683 Li, H., Rao, B., Wang, G., Shen, S., Li, D., Hu, C., Liu, Y., 2014. Spatial heterogeneity of
684 cyanobacteria-inoculated sand dunes significantly influences artificial biological soil crusts
685 in the Hopq Desert (China). Environ. Earth Sci. 71, 245–253.
686 <https://doi.org/10.1007/s12665-013-2428-6>

687 Li, P., Harding, S.E., Liu, Z., 2001. Cyanobacterial exopolysaccharides: their nature and potential
688 biotechnological applications. Biotechnol. Genet. Eng. Rev. 18, 375–404.

689 Lichner, L., Hallett, P.D., Drongová, Z., Czachor, H., Kovacik, L., Mataix-Solera, J., Homolák, M.,
690 2013. Algae influence the hydrophysical parameters of a sandy soil. CATENA, Soil Water
691 Repellency 108, 58–68. <https://doi.org/10.1016/j.catena.2012.02.016>

692 Mager, D.M., Thomas, A.D., 2010. Carbohydrates in cyanobacterial soil crusts as a source of
693 carbon in the southwest Kalahari, Botswana. Soil Biol. Biochem. 42, 313–318.
694 <https://doi.org/10.1016/j.soilbio.2009.11.009>

695 Malam Issa, O., Le Bissonnais, Y., Défarge, C., Trichet, J., 2001. Role of a cyanobacterial cover on
696 structural stability of sandy soils in the Sahelian part of western Niger. Geoderma 101, 15–
697 30. [https://doi.org/10.1016/S0016-7061\(00\)00093-8](https://doi.org/10.1016/S0016-7061(00)00093-8)

698 Malam-Issa, O., Défarge, C., Le Bissonnais, Y., Marin, B., Duval, O., Bruand, A., D'Acqui, L.P.,
699 Nordenberg, S., Annerman, M., 2007. Effects of the inoculation of cyanobacteria on the
700 microstructure and the structural stability of a tropical soil. Plant Soil 290, 209–219.

701 Mazor, G., Kidron, G.J., Vonshak, A., Abeliovich, A., 1996. The role of cyanobacterial
702 exopolysaccharides in structuring desert microbial crusts. FEMS Microbiol. Ecol. 21, 121–
703 130. <https://doi.org/10.1111/j.1574-6941.1996.tb00339.x>

704 Mugnai, G., Rossi, F., Felde, V.J.M.N.L., Colesie, C., Büdel, B., Peth, S., Kaplan, A., De Philippis,
705 R., 2018a. Development of the polysaccharidic matrix in biocrusts induced by a
706 cyanobacterium inoculated in sand microcosms. Biol. Fertil. Soils 54, 27–40.
707 <https://doi.org/10.1007/s00374-017-1234-9>

708 Mugnai, G., Rossi, F., Martin Noah Linus Felde, V.J., Colesie, C., Büdel, B., Peth, S., Kaplan, A.,
709 De Philippis, R., 2018b. The potential of the cyanobacterium *Leptolyngbya ohadii* as
710 inoculum for stabilizing bare sandy substrates. Soil Biol. Biochem. 127, 318–328.
711 <https://doi.org/10.1016/j.soilbio.2018.08.007>

712 Muñoz-Rojas, M., Román, J.R., Roncero-Ramos, B., Erickson, T.E., Merritt, D.J., Aguila-
713 Carricondo, P., Cantón, Y., 2018. Cyanobacteria inoculation enhances carbon sequestration
714 in soil substrates used in dryland restoration. Sci. Total Environ. 636, 1149–1154.
715 <https://doi.org/10.1016/j.scitotenv.2018.04.265>

- 716 Nadeau, T., Howard-Williams, C., Castenholz, R., 1999. Effects of solar UV and visible irradiance
717 on photosynthesis and vertical migration of *Oscillatoria* sp. (Cyanobacteria) in an Antarctic
718 microbial mat. *Aquat. Microb. Ecol.* 20, 231–243. <https://doi.org/10.3354/ame020231>
- 719 Ohad, I., Raanan, H., Keren, N., Tchernov, D., Kaplan, A., 2010. Light-Induced Changes within
720 Photosystem II Protects *Microcoleus* sp. in Biological Desert Sand Crusts against Excess
721 Light. *PLoS ONE* 5, e11000. <https://doi.org/10.1371/journal.pone.0011000>
- 722 Pereira, S., Zille, A., Micheletti, E., Moradas-Ferreira, P., De Philippis, R., Tamagnini, P., 2009.
723 Complexity of cyanobacterial exopolysaccharides: composition, structures, inducing factors
724 and putative genes involved in their biosynthesis and assembly. *FEMS Microbiol. Rev.* 33,
725 917–941. <https://doi.org/10.1111/j.1574-6976.2009.00183.x>
- 726 Raanan, H., Oren, N., Treves, H., Keren, N., Ohad, I., Berkowicz, S.M., Hagemann, M., Koch, M.,
727 Shotland, Y., Kaplan, A., 2016. Towards clarifying what distinguishes cyanobacteria able to
728 resurrect after desiccation from those that cannot: The photosynthetic aspect. *Biochim.*
729 *Biophys. Acta BBA - Bioenerg.* 1857, 715–722.
730 <https://doi.org/10.1016/j.bbabi.2016.02.007>
- 731 Rippka, R., 1988. Isolation and purification of cyanobacteria. *Methods Enzymol.* 167, 3–27.
- 732 Rogers, S.L., Burns, R.G., 1994. Changes in aggregate stability, nutrient status, indigenous
733 microbial populations, and seedling emergence, following inoculation of soil with *Nostoc*
734 *muscorum*. *Biol. Fertil. Soils* 18, 209–215.
- 735 Román, J.R., Rodríguez-Caballero, E., Rodríguez-Lozano, B., Roncero-Ramos, B., Chamizo,
736 S., Águila-Carricondo, P., Cantón, Y. 2019. Spectral response analysis: An indirect and non-
737 destructive methodology for the chlorophyll quantification of biocrusts. *Remote Sens.*
738 11(11),1350. <https://doi.org/10.3390/rs11111350>
- 739 Rossi, F., De Philippis, R., 2015. Role of Cyanobacterial Exopolysaccharides in Phototrophic
740 Biofilms and in Complex Microbial Mats. *Life* 5, 1218–1238.
741 <https://doi.org/10.3390/life5021218>
- 742 Rossi, F., Li, H., Liu, Y., De Philippis, R., 2017. Cyanobacterial inoculation (cyanobacterisation):
743 Perspectives for the development of a standardized multifunctional technology for soil
744 fertilization and desertification reversal. *Earth-Sci. Rev.* 171, 28–43.
745 <https://doi.org/10.1016/j.earscirev.2017.05.006>
- 746 Rossi, F., Micheletti, E., Bruno, L., Adhikary, S.P., Albertano, P., Philippis, R.D., 2012.
747 Characteristics and role of the exocellular polysaccharides produced by five cyanobacteria
748 isolated from phototrophic biofilms growing on stone monuments. *Biofouling* 28, 215–224.
749 <https://doi.org/10.1080/08927014.2012.663751>
- 750 Rossi, F., Mugnai, G., De Philippis, R., 2018. Complex role of the polymeric matrix in biological
751 soil crusts. *Plant Soil* 429, 19–34. <https://doi.org/10.1007/s11104-017-3441-4>
- 752 Rossi, F., Philippis, R.D., 2016. Exocellular Polysaccharides in Microalgae and Cyanobacteria:
753 Chemical Features, Role and Enzymes and Genes Involved in Their Biosynthesis, in:
754 Borowitzka, M.A., Beardall, J., Raven, J.A. (Eds.), *The Physiology of Microalgae,*
755 *Developments in Applied Phycology.* Springer International Publishing, pp. 565–590.
756 https://doi.org/10.1007/978-3-319-24945-2_21
- 757 Rozenstein, O., Zaady, E., Katra, I., Karnieli, A., Adamowski, J., Yizhaq, H., 2014. The effect of
758 sand grain size on the development of cyanobacterial biocrusts. *Aeolian Res.* 15, 217–226.
759 <https://doi.org/10.1016/j.aeolia.2014.08.003>
- 760 Savitzky, Abraham., Golay, M.J.E., 1964. Smoothing and Differentiation of Data by Simplified
761 Least Squares Procedures. *Anal. Chem.* 36, 1627–1639.
762 <https://doi.org/10.1021/ac60214a047>
- 763 Singh, D.P., Kaur, G., 2009. *Algal Biology and Biotechnology.* I. K. International Pvt Ltd.

- 764 Singh, J.S., Kumar, A., Rai, A.N., Singh, D.P., 2016. Cyanobacteria: A Precious Bio-resource in
765 Agriculture, Ecosystem, and Environmental Sustainability. *Front. Microbiol.* 7.
766 <https://doi.org/10.3389/fmicb.2016.00529>
- 767 Swenson, T.L., Couradeau, E., Bowen, B.P., De Philippis, R., Rossi, F., Mugnai, G., Northen, T.R.,
768 2018. A novel method to evaluate nutrient retention by biological soil crust exopolymeric
769 matrix. *Plant Soil* 429, 53–64. <https://doi.org/10.1007/s11104-017-3537-x>
- 770 Tillman, R.W., Scotter, D.R., Wallis, M.G., Clothier, B.E., 1989. Water repellency and its
771 measurement by using intrinsic sorptivity. *Soil Res.* 27, 637–644.
772 <https://doi.org/10.1071/sr9890637>
- 773 Weber, B., Olehowski, C., Knerr, T., Hill, J., Deutschewitz, K., Wessels, D.C.J., Eitel, B., Büdel,
774 B., 2008. A new approach for mapping of Biological Soil Crusts in semidesert areas with
775 hyperspectral imagery. *Remote Sens. Environ., Earth Observations for Terrestrial
776 Biodiversity and Ecosystems Special Issue* 112, 2187–2201.
777 <https://doi.org/10.1016/j.rse.2007.09.014>
- 778 Weber, B., Wu, D., Tamm, A., Ruckteschler, N., Rodríguez-Caballero, E., Steinkamp, J., Meusel,
779 H., Elbert, W., Behrendt, T., Sörgel, M., Cheng, Y., Crutzen, P.J., Su, H., Pöschl, U., 2015.
780 Biological soil crusts accelerate the nitrogen cycle through large NO and HONO emissions
781 in drylands. *Proc. Natl. Acad. Sci.* 112, 15384–15389.
782 <https://doi.org/10.1073/pnas.1515818112>
- 783 Wilde, A., Mullineaux, C.W., 2017. Light-controlled motility in prokaryotes and the problem of
784 directional light perception. *FEMS Microbiol. Rev.* 41, 900–922.
785 <https://doi.org/10.1093/femsre/fux045>

786

787

788

789

790

791 **Figure 1. Monosaccharidic composition and MW distribution of EPS produced by *L. ohadii*.** a)
792 Monosaccharide composition of RPS (dark bars) and G-EPS (white bars), expressed as internal molar %.
793 *Fuc*, fucose; *Rha*, rhamnose, *GalN*, galactosamine; *Ara*, arabinose, *GlcN*, glucosamine; *Gal*, galactose; *Glc*,
794 glucose; *Man*, mannose; *Xyl*, xylose; *Fru*, fructose; *Rib*, ribose; *GalA*, galacturonic acid; *GlcA*, glucuronic
795 acid. b) MW distribution of RPS (dark bars) and G-EPS (white bars). Different letters indicate a significant
796 difference between G-EPS and RPS ($P < 0.05$).

797

798 **Figure 2. Biomass dispersion approach and biocrusts development.** a) exemplification of the “double
799 spiral dispersion” inoculation methodology employed in this study. b) cyanobacterial biomass evenly
800 dispersed on the microcosm surface at $t = 0$; c, d) upper view of cyanobacterial biocrusts at $t = 30$ d
801 developed on MS (c) and CS (d); e, f) thickness of the cyanobacterial biocrusts on MS (e) and CS (f) at $t =$
802 30 d. MS: medium sand (granulometry 0.3 – 0.6 mm); CS: coarse sand (granulometry 0.8 – 1.25 mm).

803

804 **Figure 3. Reflectance analysis on biocrusts at t = 30 d.** Reflectance curves (average of three independent
805 replicates) of biocrusts (three inoculum amounts, 0.15, 0.45 and 0.75 mg CDW/cm²) and controls on MS (**a**)
806 and CS (**b**); spectral absorptions measured on the biocrusts and on the controls on MS (**c**) and CS (**d**).

807

808

809

810

811

812

813

814

815

816

817

818

819

820

821

822

823

824

825

826 **Table S1.** Chemical and mineralogical composition of the sand used as substrate in the microcosms.

827

Chemical composition (%)	
SiO ₂	83.3
Fe ₂ O ₃	2.1
Al ₂ O ₃	6.6
CaO	1.2
MgO	1.5
Na ₂ O	2.0
K ₂ O	2.1
Mineralogical composition (%)	
Quartz	61.8

Granitic rocks	16.5
Feldspars	12.7
Others (traces)	9.0

828
829
830
831
832
833
834
835
836
837
838
839
840
841
842
843
844
845
846
847
848
849
850
851
852
853

Table S2. Experimental design summarization. Number of microcosms employed in the two experimental phases. Phase 1: inoculation of the biomass on MS and CS microcosms; incubation for 15 and 30 d. Phase 2: Application of the sole EPS (RPS or G-EPS) in liquid suspensions to MS and CS microcosms; incubation for 30 d. Control: non-inoculated MS and CS microcosms.

Sand type	Phase 1 (biomass application)				Phase 2 (EPS application)			
	0.15 mg CDW/cm ²	0.45 mg CDW/cm ²	0.75 mg CDW/cm ²	Control	6.8 µg EPS/cm ²	13.5 µg EPS/cm ²	27.1 µg EPS/cm ²	Control
MS	6*	6*	6*	6*	6 [#]	6 [#]	6 [#]	3
CS	6*	6*	6*	6*	6 [#]	6 [#]	6 [#]	3

854
855

*3 microcosms collected and analyzed at $t = 15$ d, 3 microcosms collected and analyzed at $t = 30$ d.

[#]3 microcosms inoculated with RPS and 3 microcosms inoculated with G-EPS, all incubated for 30 days.

856

857

858

859

860

861

862

863

864

865

866

867

868

869

870

871

872

873

874

875

876

877

878

879

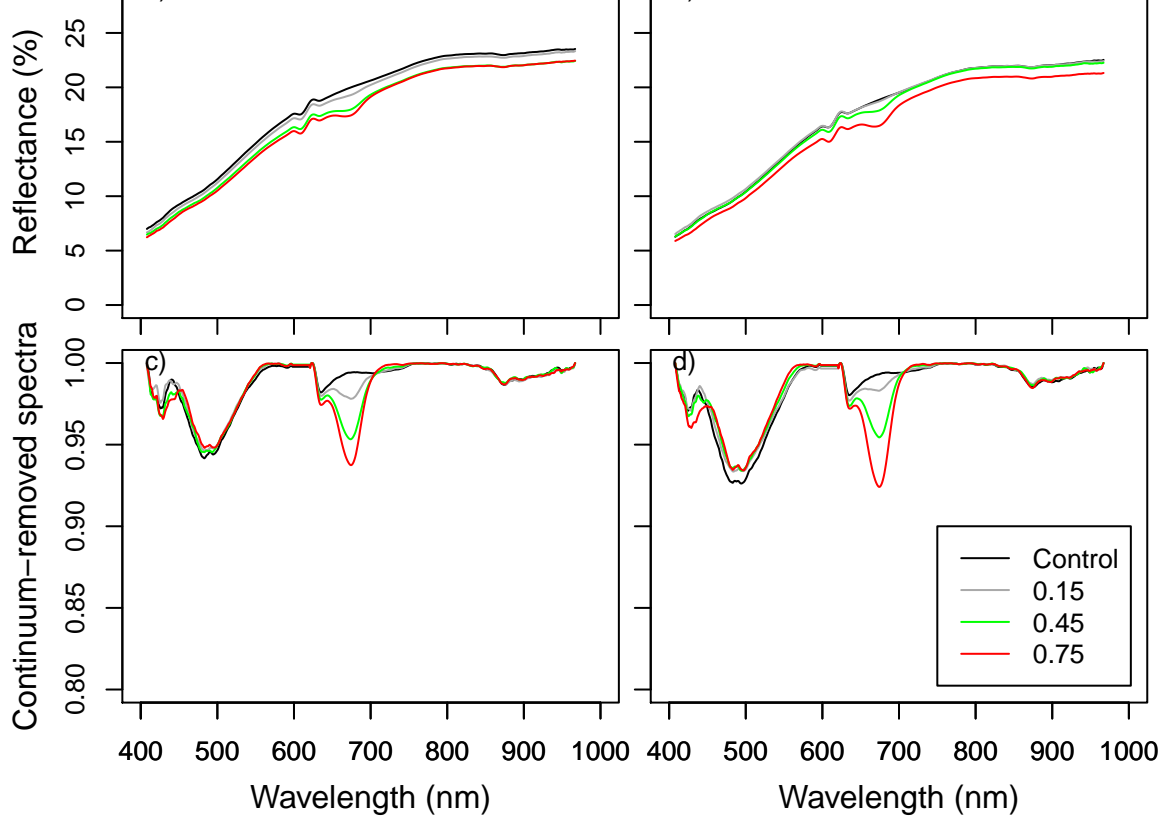
880 **Table S3.** Repellency index measured after the application of the sole EPS assessed at t = 30 d. The applied
881 quantities are expressed as microgram of EPS (RPS or G-EPS) over square centimeter of medium
882 sand (MS) or coarse sand (CS). Data are expressed as mean ± (SD).

883

EPS amount	RPS (CS)		RPS (MS)		G-EPS (CS)		G-EPS (MS)	
6.8 µg/cm ²	0.74	(0.13)	0.78	(0.04)	0.74	(0.13)	0.78	(0.04)
13.5 µg /cm ²	0.49	(0.08)	1.04	(0.26)	0.67	(0.08)	0.84	(0.04)
27.1 µg/cm ²	0.62	(0.16)	0.69	(0.09)	0.78	(0.08)	0.69	(0.06)
Control	0.71	(0.11)	0.73	(0.07)	0.71	(0.11)	0.73	(0.07)

884

- Cyanobacterization success requires an optimal initial inoculum amount
- Medium sand is more conducive to biocrust stability than coarse sand
- *L. ohadii* EPS alone cannot elicit sand aggregate stability and water repellency
- G-EPS appear as the fraction more involved in biocrust physical stability



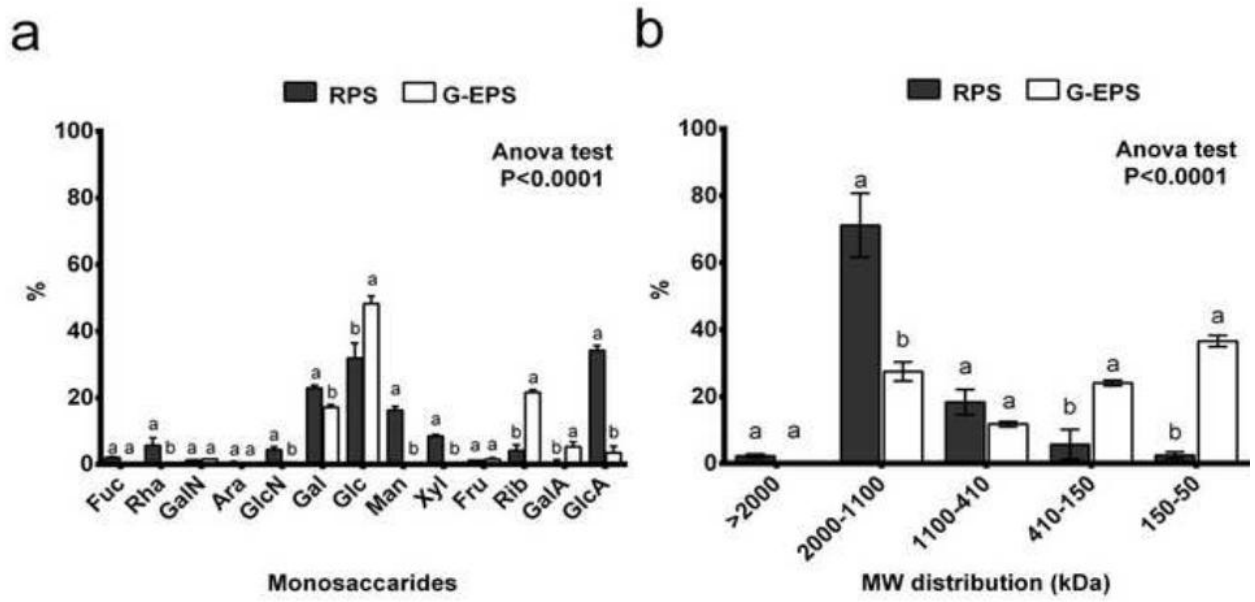


Fig. 1

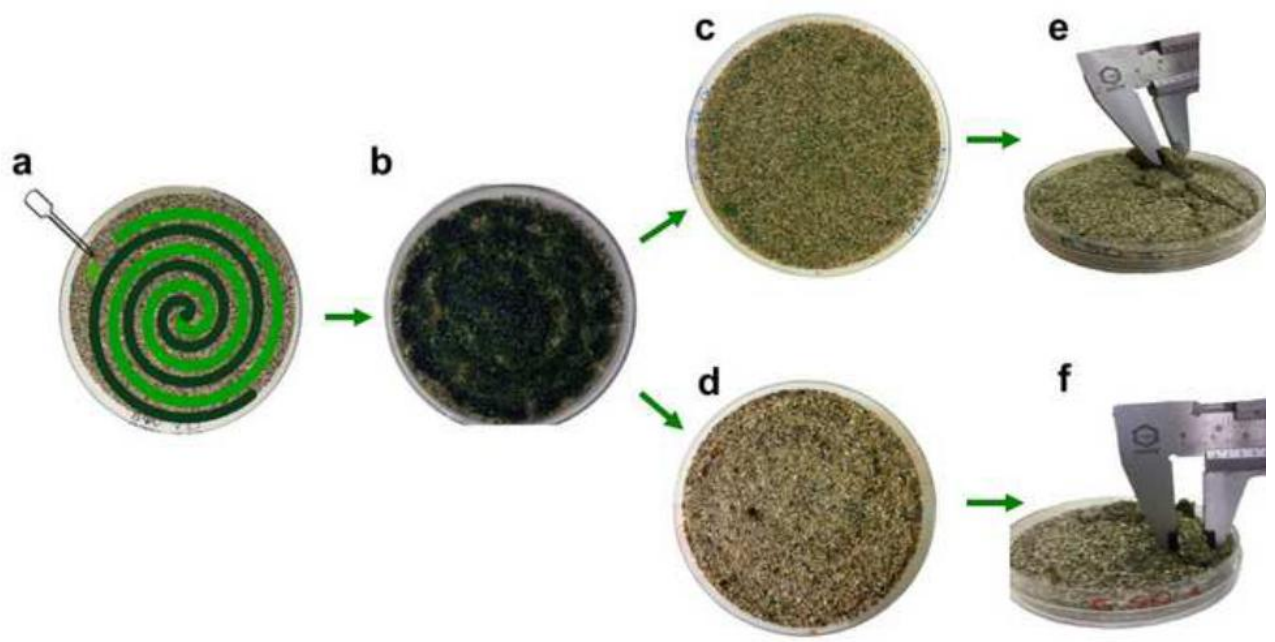


Fig. 2